On transfinite Gordon-Wixom interpolation schemes and their extensions

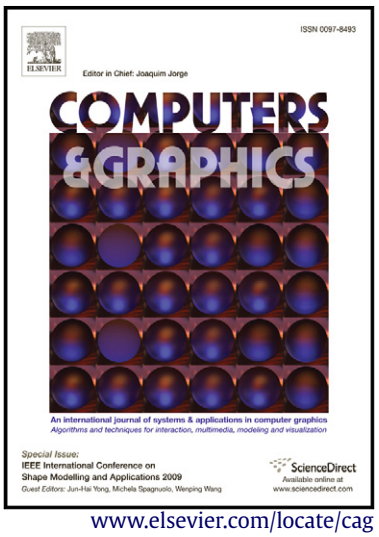

www.elsevier.com/locate/cag

On transfinite Gordon-Wixom interpolation schemes and their extensions

Alexander G. Belyaev, Pierre-Alain Fayolle

PII: S0097-8493(15)00057-6
DOI: http://dx.doi.org/10.1016/j.cag.2015.05.010
Reference: CAG2582

To appear in: *Computers & Graphics*

Received date: 12 March 2015
Revised date: 13 May 2015
Accepted date: 14 May 2015

Cite this article as: Alexander G. Belyaev, Pierre-Alain Fayolle, On transfinite Gordon-Wixom interpolation schemes and their extensions, *Computers & Graphics,* http://dx.doi.org/10.1016/j.cag.2015.05.010

On transfinite Gordon-Wixom interpolation schemes and their extensions

Alexander G. Belyaev[a], Pierre-Alain Fayolle[b]

[a]*Institute of Sensors, Signals and Systems, School of Engineering & Physical Sciences, Heriot-Watt University, Edinburgh, UK*
[b]*Computer Graphics Laboratory, University of Aizu, Aizu-Wakamatsu, Japan*

Abstract

Among various barycentric coordinates and their extensions, the linear and cubic (Hermite) Gordon-Wixom transfinite interpolation schemes deliver the most accurate approximations of the harmonic and biharmonic functions, respectively. However interpolation properties of the original Gordon-Wixom interpolations are studied for convex domains only and, therefore, their current practical importance is limited. In this paper, we propose simple modifications of the Gordon-Wixom interpolation schemes, study their properties, and show how they can be used for approximating solutions to the Poisson and inhomogeneous biharmonic equations. Our modified Gordon-Wixom interpolations are easily extended to non-convex domains and, according to our experiments, deliver more accurate approximations of the harmonic and biharmonic functions compared with the original Gordon-Wixom schemes. We also demonstrate how our approach can be used for approximating the distance function.

Keywords: Linear and cubic transfinite barycentric coordinates, pseudo-harmonic and pseudo-biharmonic interpolation schemes.

1. Introduction

In recent years, generalized barycentric coordinates have drawn a significant interest as a promising computational tool in the fields of computer graphics, image processing, and computational mathematics [1, 2, 3, 4, 5, 6, 7, 8, 9, 10]. See also references therein. While various generalized barycentric interpolation schemes were known since 1970s [11, 12], their current widespread use was initiated by seminal works of Warren [13] and Floater [14].

This paper is partially inspired by very recent applications of generalized barycentric coordinates in finite element methods [15, 16, 17, 10] where Wachspress's and Floater's mean value coordinates are considered. As the starting point of our study, we have chosen the Gordon-Wixom interpolation scheme [11] which is capable of reproducing harmonic functions if the interpolation domain is a disc (a ball in 3D). This makes the Gordon-Wixom approach potentially promising for approximating solutions of elliptic partial differential equations.

The basic idea behind the Gordon-Wixom interpolation scheme is simple and elegant. Consider a planar convex domain Ω and a function u, defined on $\partial\Omega$. Given a point $\boldsymbol{x}$ inside Ω, let us consider a straight line L_θ passing through x, making an angle θ with some fixed direction, and intersecting $\partial\Omega$ in two points $\boldsymbol{y}_1$ and $\boldsymbol{y}_2$ and use the linear interpolation between $u(\boldsymbol{y}_1)$ and $u(\boldsymbol{y}_2)$ to obtain an estimate $u(\boldsymbol{x},\theta)$ associated with direction θ. Now circular averaging of $u(\boldsymbol{x},\theta)$ w.r.t. θ yields the Gordon-Wixom interpolation of function $u(\cdot)$ from $\partial\Omega$ to $\boldsymbol{x} \in \Omega$. See Fig. 1 for an illustration.

Generalizations of the Gordon-Wixom interpolation scheme were studied in [18, 19]. In particular, Manson et al. [19] introduced a weighted circular averaging procedure which allows them to extend the Gordon-Wixom interpolation scheme into non-convex domains while keeping the weights positive. Gordon and Wixom themselves [11] extended their interpolation procedure to Hermite interpolation. Very recently Floater [20] demonstrated that their Hermite interpolation scheme reconstructs biharmonic functions in the case when the interpolation domain Ω is a disk.

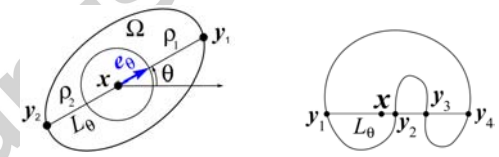

Figure 1: Left: the main idea behind the Gordon-Wixom interpolation scheme consists of combining the linear interpolation and circular averaging. Right: extending Gordon-Wixom type interpolation schemes to non-convex domains. See the main text for details.

In this paper, we consider simple modifications of the ordinary and Hermite-type Gordon-Wixom interpolation scheme and reveal their links with finite difference approximations of the Laplacian and bi-Laplacian. It allows us to demonstrate that those modified Gordon-Wixom interpolation schemes are very useful for approximating solutions to the boundary value-problems involving the Laplacian and bi-Laplacian operators. In particular, our numerical experiments show that our modifications demonstrate better approximation properties than the original Gordon-Wixom interpolation schemes.

The main tools we use to build our modifications of the linear and cubic Gordon-Wixom interpolation schemes are Taylor series expansions and certain simple mean-value formulas for the Laplacian and bi-Laplacian operators (these simple mean-

value formulas can be generalized for anisotropic diffusion operators [21, 22] which are widely used in image processing).

Results of our numerical experiments demonstrate high accuracy of the linear and cubic modified Gordon-Wixom interpolation schemes for rounded domains and domains with small diameters. Thus it seems promising to combine our interpolation schemes with polygonal finite elements for efficient numerical solving of PDEs involving the Laplacian, bi-Laplacian, and there generalizations. Another interesting application of our approach consists of using modified linear Gordon-Wixom interpolation schemes for distance function approximation, see Section 5 of this paper for details.

The rest of the paper is organized as follows. In Section 2 we introduce a modified version of the linear Gordon-Wixom interpolation scheme and extend it to non-convex domains. Section 3 is devoted to cubic (Hermite-type) Gordon-Wixom interpolation and its modification. Results of our numerical experiments are presented and discussed in Sections 4 and 5. In particular, in Section 5 we demonstrate how the modified linear Gordon-Wixom interpolation scheme can be used for approximating the distance function. We briefly conclude in Section 6.

2. Gordon-Wixom interpolation and its extensions

Let $\Omega \subset \mathbb{R}^2$ be a bounded convex domain. Given a point $\boldsymbol{x}$ inside Ω, consider the unit vector $\boldsymbol{e}_\theta$ which makes an angle θ with some prescribed direction. Let the straight line through $\boldsymbol{x}$ determined by $\boldsymbol{e}_\theta$ intersect the boundary $\partial\Omega$ in two points $\boldsymbol{y}_1$ and $\boldsymbol{y}_2$. Denote by ρ_1 and ρ_2 the distances from $\boldsymbol{x}$ to $\boldsymbol{y}_1$ and $\boldsymbol{y}_2$, respectively. Given $u(\boldsymbol{y}_1)$ and $u(\boldsymbol{y}_2)$, one can estimate $u(\boldsymbol{x})$ using the linear interpolation between $u(\boldsymbol{y}_1)$ and $u(\boldsymbol{y}_2)$

$$u(\boldsymbol{x},\theta) = \left[\frac{u(\boldsymbol{y}_1)}{\rho_1} + \frac{u(\boldsymbol{y}_2)}{\rho_2}\right] \Big/ \left[\frac{1}{\rho_1} + \frac{1}{\rho_2}\right] \tag{1}$$

Now circular averaging w.r.t. θ defines the Gordon-Wixom interpolation

$$u(\boldsymbol{x}) = \frac{1}{2\pi}\int_0^{2\pi} \left\{\left[\frac{u(\boldsymbol{y}_1)}{\rho_1} + \frac{u(\boldsymbol{y}_2)}{\rho_2}\right] \Big/ \left[\frac{1}{\rho_1} + \frac{1}{\rho_2}\right]\right\} d\theta \tag{2}$$

Pseudo-harmonic interpolation. It turns out that the Gordon-Wixom interpolation scheme is closely connected with the harmonic interpolation. Indeed, the second-order directional derivative of $u(\boldsymbol{x})$ in the $\boldsymbol{e}_\theta$-direction can be approximated by

$$\frac{\partial^2 u}{\partial \boldsymbol{e}_\theta^2}(\boldsymbol{x}) \approx \frac{2}{\rho_1\rho_2}\left\{\left[\frac{u(\boldsymbol{y}_1)}{\rho_1} + \frac{u(\boldsymbol{y}_2)}{\rho_2}\right] \Big/ \left[\frac{1}{\rho_1} + \frac{1}{\rho_2}\right] - u(\boldsymbol{x})\right\}. \tag{3}$$

Note that

$$\frac{1}{\pi}\int_0^{2\pi} \frac{\partial^2 u}{\partial \boldsymbol{e}_\theta^2}(\boldsymbol{x})\, d\theta = \frac{1}{\pi}\int_0^{2\pi} \left(\cos\theta\frac{\partial}{\partial x_1} + \sin\theta\frac{\partial}{\partial x_2}\right)^2 d\theta = \Delta.$$

Now let us approximate the second-order directional derivatives of $u(\boldsymbol{x})$ by finite differences. For $s_1, s_2 \ll 1$, the Taylor series

$$u(x+s_1) = u(x) + s_1 u'(x) + \frac{s_1^2}{2}u''(x) + \frac{s_1^3}{6}u'''(x) + \frac{s_1^4}{24}u^{(4)}(x) + \dots \tag{4}$$

$$u(x-s_2) = u(x) - s_2 u'(x) + \frac{s_2^2}{2}u''(x) - \frac{s_2^3}{6}u'''(x) + \frac{s_2^4}{24}u^{(4)}(x) + \dots \tag{5}$$

lead to the following standard approximation for $u''(\boldsymbol{x})$

$$\frac{2}{s_1 s_2}\left\{\left[\frac{u(x+s_1)}{s_1} + \frac{u(x-s_2)}{s_2}\right] \Big/ \left[\frac{1}{s_1} + \frac{1}{s_2}\right] - u(x)\right\}$$

which becomes (3) if we apply (4) and (5) in the direction defined by $\boldsymbol{e}_\theta$ and set $\rho_1 = s_1$ and $\rho_2 = s_2$.

One can hope that (3) still holds in some sense even when ρ_1 and ρ_2 are not small. Now averaging of (3) w.r.t. θ leads to an approximation of $\Delta u(\boldsymbol{x})$ by

$$\frac{1}{\pi}\int_0^{2\pi} \frac{2}{\rho_1\rho_2}\left\{\left[\frac{u(\boldsymbol{y}_1)}{\rho_1} + \frac{u(\boldsymbol{y}_2)}{\rho_2}\right] \Big/ \left[\frac{1}{\rho_1} + \frac{1}{\rho_2}\right] - u(\boldsymbol{x})\right\} d\theta.$$

Mimicking the harmonic interpolation for which

$$\Delta u(\boldsymbol{x}) = 0,$$

we arrive at the following transfinite interpolation formula

$$u(\boldsymbol{x}) = \int_0^{2\pi} \left\{\left[\frac{u(\boldsymbol{y}_1)}{\rho_1} + \frac{u(\boldsymbol{y}_2)}{\rho_2}\right] \Big/ \left[\frac{1}{\rho_1} + \frac{1}{\rho_2}\right]\right\} \frac{d\theta}{\rho_1\rho_2} \Big/ \int_0^{2\pi} \frac{d\theta}{\rho_1\rho_2} \tag{6}$$

which can be considered as a modification of the original Gordon-Wixom interpolation scheme (2).

While the boundary value interpolation property of (2) does not look obvious (it is proven rigorously in [11] for convex domains), our modification (6) can be considered as a continuous variant of the Shepard interpolation scheme [23] (interesting links between the Shepard interpolation approach and continuous barycentric coordinates were discussed in [24]). Indeed when $\boldsymbol{x} \in \Omega$ approaches $\boldsymbol{y} \in \partial\Omega$, the denominator and numerator of (6) demonstrate the following asymptotic behaviors

$$\int_0^{2\pi} \frac{d\theta}{\rho_1\rho_2} \sim \frac{C}{|\boldsymbol{x}-\boldsymbol{y}|} \quad \text{and} \quad \int_0^{2\pi} \Big\{\ \dots\ \Big\} \frac{d\theta}{\rho_1\rho_2} \sim \frac{C\,u(\boldsymbol{y})}{|\boldsymbol{x}-\boldsymbol{y}|},$$

where C is some constant. These asymptotics can be established, for example, by a technique similar to the one developed in [25].

Gordon and Wixom [11] showed that (2) reproduces an harmonic function if Ω is a circle. So does (6) because, due to the intersecting chords theorem, the product $\rho_1\rho_2$ does not depend on θ and, therefore, if Ω is a circle, (6) is reduced to (2).

While (6) is correctly defined only if Ω is convex, it is not difficult to extend it to non-convex domains by using the alternating sign procedure proposed initially by Hormann and Floater for defining the mean value coordinates in non-convex polygons [3]. For example, in the situation shown in the right image of Fig. 1 the Horman-Floater approach suggests to use

$$\left[\frac{u(\boldsymbol{y}_1)}{\rho_1} + \frac{u(\boldsymbol{y}_2)}{\rho_2} - \frac{u(\boldsymbol{y}_3)}{\rho_3} + \frac{u(\boldsymbol{y}_4)}{\rho_4}\right] \Big/ \left[\frac{1}{\rho_1} + \frac{1}{\rho_2} - \frac{1}{\rho_3} + \frac{1}{\rho_4}\right] \tag{7}$$

instead of the expression in the curly braces in (6) and

$$\frac{1}{\rho_1}\left(\frac{1}{\rho_2} - \frac{1}{\rho_3} + \frac{1}{\rho_4}\right) \tag{8}$$

instead of $1/(\rho_1\rho_2)$ in (6).

Another approach to extend (6) and similar schemes to non-convex domains consists of considering only the first intersections of L_θ with $\partial\Omega$, as suggested in [26]. For the above example, it means using $u(\boldsymbol{y}_1)/\rho_1 + u(\boldsymbol{y}_2)/\rho_2$ and $1/(\rho_1\rho_2)$ instead of (7) and (8), respectively.

Pseudo-Poisson interpolation. Assume now that we want to approximate the solution to

$$-\Delta u = f(\boldsymbol{x}) \quad \text{for } \boldsymbol{x} \in \Omega, \qquad u(\boldsymbol{y}) = g(\boldsymbol{y}) \quad \text{for } \boldsymbol{y} \in \partial\Omega. \tag{9}$$

Similar to the above, using (3) to approximate Δu, we arrive at

$$u(\boldsymbol{x}) = \frac{\pi}{2} f(\boldsymbol{x}) \left/ \int_0^{2\pi} \frac{d\theta}{\rho_1\rho_2} \right. + \int_0^{2\pi} \left\{ \left[\frac{g(\boldsymbol{y}_1)}{\rho_1} + \frac{g(\boldsymbol{y}_2)}{\rho_2} \right] \middle/ \left[\frac{1}{\rho_1} + \frac{1}{\rho_2} \right] \right\} \frac{d\theta}{\rho_1\rho_2} \left/ \int_0^{2\pi} \frac{d\theta}{\rho_1\rho_2} \right. \tag{10}$$

In particular, assuming that $u(\boldsymbol{x}) = 0$ on $\partial\Omega$ and $f(\boldsymbol{x}) \equiv 1$ yields

$$u(\boldsymbol{x}) = \left(\frac{2}{\pi} \int_0^{2\pi} \frac{d\theta}{\rho_1\rho_2} \right)^{-1} \tag{11}$$

If Ω is a circle of radius R then the solution to (9) with $g \equiv 0$ and $f(\boldsymbol{x}) \equiv 1$ is given by $\left(R^2 - \boldsymbol{x}^2\right)/4$. The same expression is obtained from (11) because, according to the intersection chords theorem,

$$\rho_1\rho_2 = (R - |\boldsymbol{x}|)(R + |\boldsymbol{x}|) = R^2 - |\boldsymbol{x}|^2.$$

Thus, taking into account that (6) reproduces harmonic functions if Ω is a disk, we arrive at the following result.

Proposition 1. Let Ω be a disk and $f \equiv \text{const}$ in Ω. Then (10) delivers the exact solution to (9).

3. Hermite-type Gordon-Wixom interpolation

In their paper [11], Gordon and Wixom extended their approach to Hermite type interpolation. Similar to the linear case, the cubic Gordon-Wixom interpolation scheme combines directional interpolation with angular averaging. Namely, consider a planar convex domain Ω, a point $\boldsymbol{x}$ inside Ω, a straight line L_θ passing through $\boldsymbol{x}$, intersecting $\partial\Omega$ in two points $\boldsymbol{y}_1$ and $\boldsymbol{y}_2$, and making an angle θ with some fixed direction. The cubic interpolation along L_θ yields

$$u(\boldsymbol{x},\theta) = \frac{(3\rho_1+\rho_2)\rho_2^2}{(\rho_1+\rho_2)^3} u(\boldsymbol{y}_1) + \frac{(\rho_1+3\rho_2)\rho_1^2}{(\rho_1+\rho_2)^3} u(\boldsymbol{y}_2) - \frac{\rho_1\rho_2^2}{(\rho_1+\rho_2)^2} u'(\boldsymbol{y}_1) + \frac{\rho_1^2\rho_2}{(\rho_1+\rho_2)^2} u'(\boldsymbol{y}_2), \tag{12}$$

where the derivatives are taken in the direction of $\boldsymbol{e}_\theta$. Now averaging of the above expression w.r.t. θ leads to the cubic Gordon-Wixom interpolation scheme

$$u(\boldsymbol{x}) = \frac{1}{2\pi} \int_0^{2\pi} u(\boldsymbol{x},\theta)\, d\theta. \tag{13}$$

This transfinite interpolation scheme possesses remarkable properties: it has cubic precision (reproduces cubic bivariate polynomials from their values on $\partial\Omega$) and, in addition, reproduces biharmonic functions if Ω is a disk.

This biharmonic reproduction property for (12), (13) was conjectured in [11] and rigorously proved in [20]. Below we investigate the link between (12), (13) and the biharmonic operator Δ^2, the so-called bi-Laplacian, in detail.

Approximate bi-Laplacian via circular averaging. In addition to Taylor series (4) and (5) let us also consider similar expansions for the first-order derivatives

$$u'(x+s_1) = u'(x) + s_1 u''(x) + \frac{s_1^2}{2} u'''(x) + \frac{s_1^3}{6} u^{(4)}(x) + \dots, \tag{14}$$

$$u'(x-s_2) = u'(x) - s_2 u''(x) + \frac{s_2^2}{2} u'''(x) - \frac{s_2^3}{6} u^{(4)}(x) + \dots, \tag{15}$$

where as usual we assume that $s_1, s_2 \ll 1$. Taking the sum of

(4) with weight $w_1 = s_2^2(3s_1 + s_2)/(s_1 + s_2)^3$,
(5) with weight $w_2 = s_1^2(s_1 + 3s_2)/(s_1 + s_2)^3$,
(14) with weight $w_3 = -s_1 s_2^2/(s_1 + s_2)^2$,
(15) with weight $w_4 = s_1^2 s_2/(s_1 + s_2)^2$,

respectively, we arrive at

$$u(x) - \frac{s_1^2 s_2^2}{24} u^{(4)}(x) + \text{higher-order terms}.$$

Thus we have for the 4th-order derivative

$$u^{(4)}(x) \approx \frac{24}{s_1^2 s_2^2} \left[u(x) - w_1 u(x+s_1) - w_2 u(x-s_2) - w_3 u'(x+s_1) - w_4 u'(x-s_2) \right]$$

Now let us approximate the 4th-order directional derivative of $u(\boldsymbol{x})$ in the direction $\boldsymbol{e}_\theta$ by

$$\frac{\partial^4 u}{\partial \boldsymbol{e}_\theta^4}(\boldsymbol{x}) \approx \frac{24}{\rho_1^2\rho_2^2} \left[u(\boldsymbol{x}) - \frac{(3\rho_1+\rho_2)\rho_2^2}{(\rho_1+\rho_2)^3} u(\boldsymbol{y}_1) - \frac{(\rho_1+3\rho_2)\rho_1^2}{(\rho_1+\rho_2)^3} u(\boldsymbol{y}_2) + \frac{\rho_1\rho_2^2}{(\rho_1+\rho_2)^2} u'(\boldsymbol{y}_1) - \frac{\rho_1^2\rho_2}{(\rho_1+\rho_2)^2} u'(\boldsymbol{y}_2) \right] \tag{16}$$

One can easily check that

$$\frac{4}{3\pi} \int_0^{2\pi} \left(\frac{\partial^4 u}{\partial \boldsymbol{e}_\theta^4} \right) d\theta = \Delta^2 u. \tag{17}$$

Combining (16) and (17) for approximating the solution to the biharmonic equation

$$\Delta^2 u = 0 \quad \text{in} \quad \Omega$$

accompanied by the standard Dirichlet boundary conditions we arrive at

$$u(\boldsymbol{x}) = \int_0^{2\pi} \left\{ \frac{(3\rho_1+\rho_2)\rho_2^2}{(\rho_1+\rho_2)^3} u(\boldsymbol{y}_1) + \frac{(\rho_1+3\rho_2)\rho_1^2}{(\rho_1+\rho_2)^3} u(\boldsymbol{y}_2) \right. \tag{18}$$

$$- \frac{\rho_1\rho_2^2}{(\rho_1+\rho_2)^2}\frac{\partial u}{\partial \boldsymbol{e}_\theta}(\boldsymbol{y}_1) + \frac{\rho_1^2\rho_2}{(\rho_1+\rho_2)^2}\frac{\partial u}{\partial \boldsymbol{e}_\theta}(\boldsymbol{y}_2)\Big\}\frac{d\theta}{\rho_1^2\rho_2^2}\Big/\int_0^{2\pi}\frac{d\theta}{\rho_1^2\rho_2^2}$$

which yields a simple modification of the cubic Gordon-Wixom interpolation scheme. This modification also has a cubic precision and, in view of the intersection chords theorem, reproduces biharmonic functions if Ω is a disk. In addition, similar to the Laplacian case, (18) can be easily extended to non-convex domains.

Approximate solution to the inhomogeneous biharmonic equation. Similar to the Laplacian case, we can use (16), (17) to approximate the solution to an inhomogeneous biharmonic equation. We can restrict ourselves to considering the homogeneous Dirichlet boundary conditions for

$$\Delta^2 u = f(\boldsymbol{x}) \quad \text{for } \boldsymbol{x} \in \Omega, \tag{19}$$

as the case $f \equiv 0$ with inhomogeneous Dirichlet boundary conditions is approximated by (18).

Now (16), (17) together with the homogeneous Dirichlet boundary conditions (i.e., $u(\boldsymbol{x})$ and its gradient vanish on $\partial\Omega$) yields the approximation

$$u(\boldsymbol{x}) = \frac{\pi}{32} f(\boldsymbol{x}) \Big/ \int_0^{2\pi} \frac{d\theta}{\rho_1^2\rho_2^2} \tag{20}$$

Interestingly, similar to the Laplacian case considered earlier, if Ω is a disk, then (20) with $f \equiv$ const reproduces the true solution to (19) subject to the homogeneous Dirichlet boundary conditions. Namely, if $\Omega = \{|\boldsymbol{x}| < R\}$ and $f \equiv 1$, then both (19) and (20) produce the same result: $u(\boldsymbol{x}) = (R^2 - |\boldsymbol{x}|^2)^2/64$.

4. Numerical experiments

Implementation. Evaluation of the Gordon-Wixom interpolants (6), (10), (18) or (20) requires the computation of integrals over $[0, 2\pi]$. In our experiments, these integrals are evaluated numerically using the composite trapezoidal rule with n subintervals. Quantitatively, the residual norm of the approximation given by (10) w.r.t the exact solution $u(\boldsymbol{x}) = (4 - \boldsymbol{x}^2)/4$ of $-\Delta u = 1$ on a unit disk is given in Table 1 for different number of integration points. In all the experiments below, we use $n = 100$ subintervals, which delivers a sufficiently good approximation for the considered domains.

	$\|u - \tilde{u}\|_2$
5 points	$5.082\ \ 10^{-2}$
10 points	$2.541\ \ 10^{-2}$
50 points	$5.082\ \ 10^{-3}$
100 points	$2.541\ \ 10^{-3}$

Table 1: Residual $\|u-\tilde{u}\|_2$ for the modified Gordon-Wixom interpolation ($\tilde{u}$) approximating the solution of $-\Delta u = 1$ for the disk domain with different number of integration points.

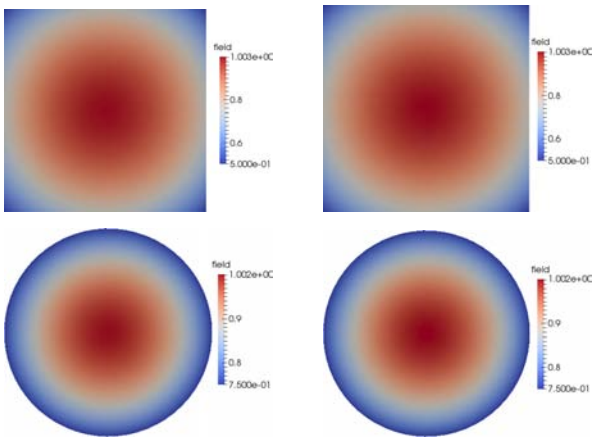

Figure 2: Comparison between an exact solution to $-\Delta u = 1$ and the Gordon-Wixom interpolation. Left: Exact solution; Right: Solution obtained by (10).

Pseudo-Poisson interpolation. We consider first applying (10) to compute an approximation to the solution of the Poisson problem with Dirichlet boundary conditions (9). For the particular case $f(\boldsymbol{x}) \equiv 1$, an exact solution is given by: $u(\boldsymbol{x}) = (R^2 - \boldsymbol{x}^2)/4$, for some value of R. We use $R = 2$ below. Boundary conditions are obtained by evaluating the known solution on the domain boundary. Figure 2 compares the exact solution (left) to the solution obtained by the Gordon-Wixom interpolant (10), right image, on convex domains (a unit disk and a square with length 2). In both cases, the interpolant delivers a very good approximation of the exact solution. This is confirmed by the plot of the point-wise error $|u - \tilde{u}|$ in Fig. 3, where u is the exact solution and $\tilde{u}$ the approximation obtained by the modified Gordon-Wixom scheme. Table 3 shows the residual norm $\|u - \tilde{u}\|_2$ for these domains. Similar results are obtained for the L_1 and L_∞ norms. This shows that the modified Gordon-Wixom interpolant delivers a good approximation.

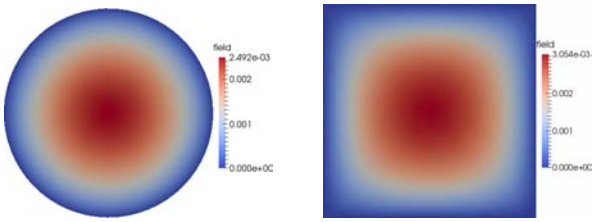

Figure 3: Absolute error for the approximation of $-\Delta u = 1$ by the modified Gordon-Wixom scheme.

Approximate solution to the inhomogeneous biharmonic equation. Similarly we can use the results of Section 3 to compute an approximate solution to the inhomogeneous biharmonic equation (19) with given boundary conditions. To verify the approximation quality, we consider the particular case $f(\boldsymbol{x}) \equiv 1$ for which an exact solution is given by $u(\boldsymbol{x}) = (R^2 - \boldsymbol{x}^2)^2/64$. We use $R = 2$ in the computations below. The point-wise error between the solution obtained by the modified Gordon-Wixom interpolation and an exact solution is shown in Fig. 4. Quantitatively, the L_2 norm of the residual is given in Table 2 for the

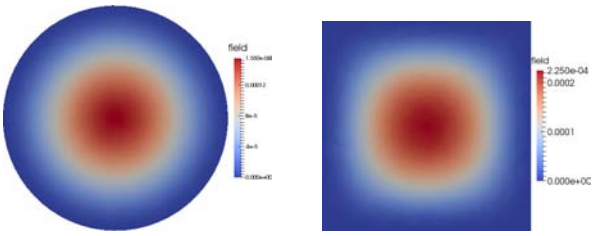

Figure 4: Absolute errors for the approximation of $\Delta^2 u = 1$ with the modified Gordon-Wixom scheme.

same domains. It shows that the interpolation schemes deliver again a very good approximation of the exact solution for the case of the inhomogeneous biharmonic equation.

	$\|u - \tilde{u}\|_2$
Disk	$1.227\ 10^{-4}$
Square	$1.976\ 10^{-4}$

Table 2: Residual norm $\|u - \tilde{u}\|_2$ for the modified Gordon-Wixom interpolation ($\tilde{u}$) approximating the solution of $\Delta^2 u = 1$.

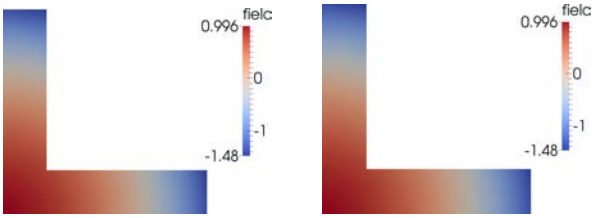

Figure 5: Comparison between an exact solution to $-\Delta u = 1$ and the Gordon-Wixom interpolation on a non-convex domain. Left: Exact solution; Right: Solution obtained by (10).

Approximation on non-convex domains. While the interpolation schemes are derived for convex domains, we can experiment to see how they behave on non-convex domains. In Fig. 5, the exact solution $u(\boldsymbol{x}) = (4 - \boldsymbol{x}^2)/4$ for the Poisson equation $-\Delta u = 1$ is compared on a convex domain to the approximation given by (10). For a convex domain, $\pm \boldsymbol{e}_\theta$ may intersect the boundary at more than one point, we use for $\boldsymbol{y}_1$ (respectively $\boldsymbol{y}_2$) the closest intersection point in the direction $\boldsymbol{e}_\theta$ (respectively $-\boldsymbol{e}_\theta$). In spite of the domain being concave, the approximation is still very good. This is confirmed quantitatively by the residual norm given in Table 3.

	$\|u - \tilde{u}\|_2$
Disk	$2.541\ 10^{-3}$
Square	$3.418\ 10^{-3}$
L shape	$6.936\ 10^{-4}$
U shape	$7.766\ 10^{-4}$

Table 3: Residual $\|u - \tilde{u}\|_2$ for the modified Gordon-Wixom interpolation ($\tilde{u}$) approximating the solution of $-\Delta u = 1$.

Comparison against the original Gordon-Wixom interpolation scheme. Figure 6 shows the point-wise error for the approximations obtained by the original (2), top images, and the modified (6), bottom images, Gordon-Wixom interpolation against an exact solution ($u(x, y) = x^3 - 3xy^2$) for the Laplace equation: $\Delta u = 0$. Table 4 gives the residual norms for both schemes. From our experiments, the modified Gordon-Wixom scheme (6) yields better results than the original scheme (2). Additionally, as described and demonstrated above, the modified Gordon-Wixom scheme can be used to provide approximate solutions to Poisson and inhomogeneous biharmonic equations.

	original GW	modified GW
Disk	$4.885\ 10^{-3}$	$4.439\ 10^{-5}$
Square	$2.926\ 10^{-1}$	$7.530\ 10^{-2}$
L	1.497	$6.295\ 10^{-2}$
U	1.978	$4.386\ 10^{-2}$

Table 4: Residual $\|u - \tilde{u}\|_2$ for the original and the modified Gordon Wixom interpolation approximating the solution of $\Delta u = 0$.

Influence of the domain size.. Since the modified Gordon-Wixom interpolation schemes are derived from Taylor series approximations, it is interesting to look at the influence of the domain size on the approximation error. In the following, the previous domains are uniformly scaled by 10. Tables 5 and 6 give the residual norms for the Laplace equation $\Delta u = 0$ and the Poisson equation $-\Delta u = 1$ for the different domain sizes. The same number of integration points (100) is used for evaluating the integrals for both domain sizes (original and scaled). As the domain size increases, the error increases as well. Increasing the number of integration points allows to decrease the error, but at the expense of speed.

	Original domain	Scaled domain
Disk	$4.439\ 10^{-5}$	$4.439\ 10^{-1}$
Square	$7.530\ 10^{-2}$	$7.530\ 10^{2}$
L	$6.295\ 10^{-2}$	$6.295\ 10^{2}$
U	$4.386\ 10^{-2}$	$4.386\ 10^{2}$

Table 5: Residual $\|u - \tilde{u}\|_2$ for the modified Gordon-Wixom interpolation ($\tilde{u}$) approximating the solution of $\Delta u = 0$ for a domain and its uniformly scaled version by 10.

	Original domain	Scaled domain
Disk	$2.541\ 10^{-3}$	2.541
Square	$3.418\ 10^{-3}$	3.418
L	$6.936\ 10^{-4}$	$6.936\ 10^{-1}$
U	$7.766\ 10^{-4}$	$7.766\ 10^{-1}$

Table 6: Residual $\|u - \tilde{u}\|_2$ for the modified Gordon-Wixom interpolation ($\tilde{u}$) approximating the solution of $-\Delta u = 1$ for a domain and its uniformly scaled version by 10.

5. Application to distance function approximation

In this section, we demonstrate briefly how linear modified Gordon-Wixom interpolation schemes can be used for distance function approximation purposes. Efficient computation of the

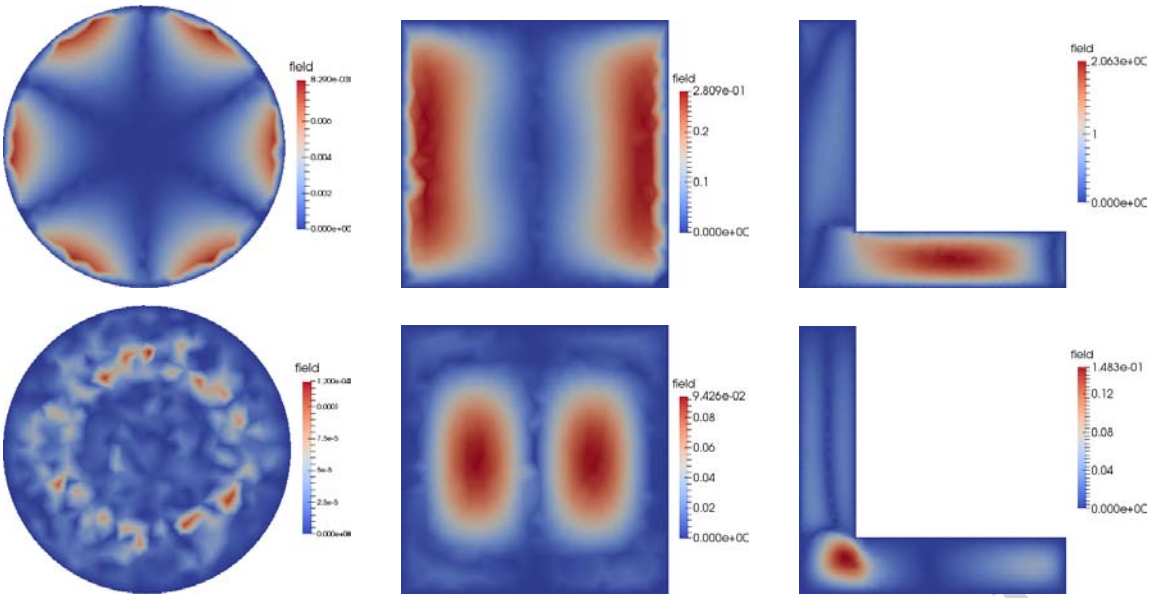

Figure 6: Absolute error for the approximation of $\Delta u = 0$ by the original (top) and the modified (bottom) Gordon-Wixom scheme.

distance fields and their approximations is important for a number of shape modeling applications including editing [27, 28], heterogeneous material modeling [29], modeling of complex geometric patterns [30], and surface reconstruction from scattered point data [31].

A simple yet efficient approach for a distance function approximation was proposed by Spalding [32] and further developed by Tucker [33] in connection to their studies of turbulence phenomena [34] (see also references therein). The approach consists of solving the Poisson equation

$$\Delta u = -1 \quad \text{in} \quad \Omega, \qquad u(\boldsymbol{x}) = 0 \quad \text{on} \quad \partial\Omega \tag{21}$$

and then applying a normalization procedure to $u(\boldsymbol{x})$

$$v(\boldsymbol{x}) = \sqrt{|\nabla u|^2 + 2u} - |\nabla u| = \frac{2u}{|\nabla u| + \sqrt{|\nabla u|^2 + 2u}}. \tag{22}$$

Then $v(\boldsymbol{x})$ delivers a highly accurate approximation of $\mathrm{dist}(\boldsymbol{x}, \partial\Omega)$ near $\partial\Omega$.

Practically, (21) is solved by meshing the domain and using finite element analysis. Instead, we can use (10) as an approximation of the solution to (21). The main advantage of (10) is that, in contrast to (21), it is local: we can independently compute (10) for each $\boldsymbol{x} \in \Omega$. Thus approximation (10) with $f(\boldsymbol{x}) \equiv 1$ can be used instead of (21) if one needs to estimate the distance in a region of interest near $\partial\Omega$.

Fig. 7 presents results of our numerical experiments with approximating the distance function $\mathrm{dist}(\boldsymbol{x}, \partial\Omega)$ by (10) and (22) for a geometrically complex domain. One can observe that our approach deliver a very accurate approximation for $\mathrm{dist}(\boldsymbol{x}, \partial\Omega)$ near $\partial\Omega$.

6. Conclusion

In this paper, we have demonstrated how the Gordon-Wixom interpolation approach can be extended to approximate solutions to homogeneous and inhomogeneous harmonic (Laplace and Poisson) and biharmonic equations. Although the considered approximations are not expected to be accurate everywhere in an arbitrary domain, they fairly reproduce the behaviors of the true solutions. So the considered boundary value interpolations can be used as initial approximations for iterative PDE solvers. In addition, our approximations become more and more accurate, as the size of the domain decreases. So we hope that the proposed approximations can find applications in finite element schemes developed for solving boundary value problems for elliptic PDEs involving the Laplacian and bi-Laplacian operators. As an immediate application of our approach, we show how it can be used for approximating the distance function.

Acknowledgements. We would like to thank the SMI 2015 reviewers of our paper for their encouraging, valuable, and constructive comments.

References

[1] Meyer M, Barr A, Lee H, Desbrun M. Generalized barycentric coordinates on irregular polygons. Journal of Graphics Tools 2002;7(1):13–22.

[2] Ju T, Schaefer S, Warren J. Mean value coordinates for closed triangular meshes. ACM Transactions on Graphics 2005;24(3):561–6. Proceedings of ACM SIGGRAPH 2005.

[3] Hormann K, Floater MS. Mean value coordinates for arbitrary planar polygons. ACM Transactions on Graphics 2006;25(4):1424–41.

[4] Sukumar N, Malsch EA. Recent advances in the construction of polygonal finite element interpolants. Archives of Computational Methods in Engineering 2006;13(1):129–63.

[5] Schaefer S, McPhail T, Warren J. Image deformation using moving least squares. ACM Transactions on Graphics 2006;25(3):533–40. Proceedings of ACM SIGGRAPH 2006.

[6] Joshi P, Meyer M, DeRose T, Green B, Sanocki T. Harmonic coordinates for character articulation. ACM Transactions on Graphics 2007;26(3):71:1–10. Proceedings of ACM SIGGRAPH 2007.

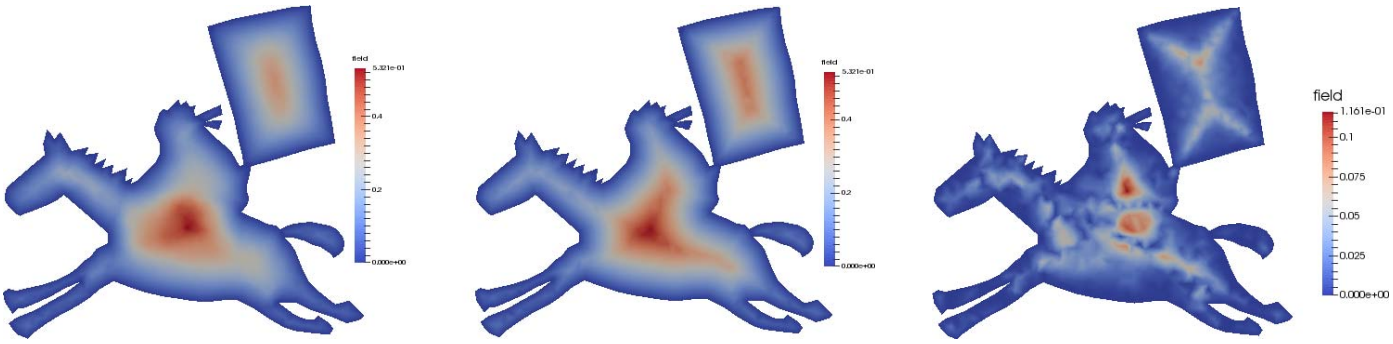

Figure 7: Left: distance function approximation by (10) with $f(\boldsymbol{x}) \equiv 1$ followed by normalization (22). Middle: the exact distance function $\mathrm{dist}(\boldsymbol{x}, \partial\Omega)$. Right: the approximation error, notice how accurate the approximation is near $\partial\Omega$.

[7] Lipman Y, Levin D, Cohen-Or D. Green coordinates. ACM Transactions on Graphics 2008;27(3):78:1–10. Proceedings of ACM SIGGRAPH 2008.

[8] Farbman Z, Hoffer G, Lipman Y, Cohen-Or D, Lischinski D. Coordinates for instant image cloning. ACM Transactions on Graphics 2009;28(3):67:1–9. Proceedings of ACM SIGGRAPH 2009.

[9] Li XY, Ju T, Hu SM. Cubic mean value coordinates. ACM Transactions on Graphics 2013;32(4):126:1–10. Proceedings of ACM SIGGRAPH 2013.

[10] Manzini G, Russo A, Sukumar N. New perspectives on polygonal and polyhedral finite element methods. Math Models Methods Appl Sci 2014;24(8):1665–99.

[11] Gordon W, Wixom J. Pseudo-harmonic interpolation on convex domains. SIAM J Numer Anal 1974;11(5):909–33.

[12] Wachspress EL. A Rational Finite Element Basis. New York: Academic Press; 1975.

[13] Warren J. Barycentric coordinates for convex polytopes. Advances in Computational Mathematics 1996;6(2):97–108.

[14] Floater MS. Mean value coordinates. Computer Aided Geometric Design 2003;20(1):19–27.

[15] Gillette A, Rand A, Bajaj C. Error estimates for generalized barycentric interpolation. Advances in computational mathematics 2012;37(3):417–39.

[16] Rand A, Gillette A, Bajaj C. Interpolation error estimates for mean value coordinates over convex polygons. Advances in computational mathematics 2013;39(2):327–47.

[17] Floater MS, Gillette A, Sukumar N. Gradient bounds for Wachspress coordinates on polytopes. SIAM J Numer Anal 2014;52:515–32.

[18] Belyaev A. On transfinite barycentric coordinates. In: SGP 2006: Proceedings of the fourth Eurographics Symposium on Geometry Processing. 2006, p. 89–99.

[19] Manson J, Li K, Schaefer S. Positive Gordon-Wixom coordinates. Computer-Aided Design 2011;43(11):1422–6.

[20] Floater MS. Generalized barycentric coordinates and applications. Acta Numerica 2015;.

[21] Weickert J. Anisotropic diffusion filters for image processing based quality control. In: Proc. Seventh European Conf. on Mathematics in Industry. Teubner-Verlag; 1994, p. 355–62.

[22] Weickert J, Scharr H. A scheme for coherence-enhancing diffusion filtering with optimized rotation invariance. Journal of Visual Communication and Image Representation 2002;13:103–18.

[23] Shepard D. A two-dimensional interpolation function for irregularly-spaced data. In: Proceedings of the 1968 23rd ACM national conference. 1968, p. 517–24.

[24] Schaefer S, Ju T, Warren J. A unified, integral construction for coordinates over closed curves. Computer Aided Geometric Design 2007;24(8-9):481–93.

[25] Belyaev A, Fayolle PA, Pasko A. Signed L_p-distance fields. Computer-Aided Design 2013;45:523–8.

[26] Lipman Y, Kopf J, Cohen-Or D, Levin D. GPU-assisted positive mean value coordinates for mesh deformations. In: SGP 2007: Proceedings of the fifth Eurographics Symposium on Geometry Processing. 2007, p. 117–24.

[27] Breen DE, Whitaker RT. A level-set approach for the metamorphosis of solid models. Visualization and Computer Graphics, IEEE Transactions on 2001;7(2):173–92.

[28] Museth K, Breen DE, Whitaker RT, Barr AH. Level set surface editing operators. ACM Transactions on Graphics (TOG) 2002;21(3):330–8.

[29] Biswas A, Shapiro V, Tsukanov I. Heterogeneous material modeling with distance fields. Comput Aided Geom Des 2004;21:215–42.

[30] Peng J, Kristjansson D, Zorin D. Interactive modeling of topologically complex geometric detail. ACM Trans Graph 2004;23:635–43. ACM SIGGRAPH 2004.

[31] Calakli F, Taubin G. SSD: smooth signed distance surface reconstruction. Computer Graphics Forum 2011;30(7):1993–2002.

[32] Spalding DB. Calculation of turbulent heat transfer in cluttered spaces. In: Proc. 10th Int. Heat Transfer Conference. Brighton, UK; 1994,.

[33] Tucker PG. Assessment of geometric multilevel convergence and a wall distance method for flows with multiple internal boundaries. Applied Mathematical Modelling 1998;22:293–311.

[34] Tucker PG. Unsteady Computational Fluid Dynamics in Aeronautics. Springer; 2014.